

**SIMULATION OF AIRBORNE ELECTROMAGNETIC MEASUREMENTS IN
THREE DIMENSIONAL ENVIRONMENTS**

David L. Alumbaugh and Gregory A. Newman
Sandia National Laboratories
P.O. Box 5800 MS 0750
Albuquerque, NM 87185-0750,

Conf-950450--4

*This work was performed at Sandia National Laboratories, which is operated for the United States Department of Energy under contract number DE-AC04-94AL85000.

ABSTRACT

A 3-D frequency domain EM modeling code has been implemented for helicopter electromagnetic (HEM) simulations. A vector Helmholtz formulation for the electric fields is employed to avoid problems associated with the first order Maxwell's equations numerically decoupling in the air. Additional stability is introduced by formulating the problem in terms of the scattered electric fields which replaces an impressed dipole source with an equivalent source that possesses a much smoother spatial dependence and is easier to model. In order to compute this equivalent source, a primary field arising from dipole sources in a whole space must be calculated where ever the conductivity is different than that of the background.

The Helmholtz equation is approximated using finite differences on a staggered grid. After finite differencing, a complex-symmetric matrix system of equations is assembled and preconditioned using Jacobi scaling before it is solved using the quasi-minimum residual (QMR) method. In order to both speed up the solution and allow for larger, more realistic models to be simulated, the scheme has been modified to run on massively parallel architectures. The solution has been compared against other 1-D and 3-D numerical models and is found to produce results in good agreement. The versatility of the scheme is demonstrated by simulating a survey over a salt water intrusion zone in the Florida Everglades.

INTRODUCTION

With the increasing use of helicopter electromagnetic (HEM) methods for mapping hazardous waste sites comes the need for more rigorous forms of interpretation. Models of isolated targets such as buried plate or spheres embedded in layered half spaces (Palacky and West, 1991) are useful only for simple interpretation. The advances made over the last decade with three-dimensional (3-D) integral equation (IE) solutions (Tripp and Hohmann, 1984; Newman et al., 1986 and Xiong, 1992) has allowed the relatively quick calculation of more generally shaped 3-D bodies located in a layered media. Unfortunately the solution time for an integral equation scheme goes as order $27N^3$, where N is the number of cells representing the structure. Thus IE solutions are only practical for compact bodies. To efficiently model the response of realistic 2-D and 3-D earth structures in the presence of surface topography, differential equation (DE) solutions to Maxwell's equations must be employed.

Even with the ability to model general structures using DE methods, the calculation of HEM responses on traditional serial computers is limited. This is due to the fact that in an airborne survey the source is constantly moving and the data are collected at several frequencies. Because each new source position and frequency requires a new forward model to be calculated, the simulation of even only a small part of an airborne survey may require the solution of tens, hundreds or even thousands of forward models. To partially overcome this limitation more powerful massively parallel computers can be employed. This allows us to simulate airborne EM data that would take a few days or longer in a matter of a few hours or even minutes, thus minimizing the turn around time for interpretation.

In this paper we will show how to simulate HEM responses to geologic structure using the method of finite differences (FD) on massively parallel computers. First the theoretical basis of our FD-DE solution will be developed. Next the methods employed to numerically solve the FD problem will briefly be examined. Checks on the solution will then be presented for a simple half-space and a compact 3-D target. Finally the capability of the new modeling approach is realized with the simulation of an airborne survey over a sea water intrusion site in Florida.

DISTRIBUTION OF THIS DOCUMENT IS UNLIMITED

MASTER

DISCLAIMER

Portions of this document may be illegible in electronic image products. Images are produced from the best available original document.

THEORETICAL DEVELOPMENT

The FD solution that we have developed for computing HEM responses on serial computers is outlined in Alumbaugh and Newman (1994). However, for completeness we have included a brief description of its development here.

The HEM responses we are interested in simulating require that a magnetic dipole source is located in close proximity to the receiver. This severely complicates matters for the finite difference solution of the total field because the fields in the vicinity of the source are rapidly varying. If too coarse a mesh is used, numerical differencing at the receiver will be prone to inaccuracies. On the other hand, employing a very fine grid near the source and receiver limits the size of the model to be calculated due to storage overhead. To avoid these problems, we have chosen to work with the scattered field versions of Maxwell's equations which have the form

$$\nabla \times \mathbf{E}_s = -i\omega\mu\mathbf{H}_s + (\mu - \mu_p)\mathbf{H}_p \quad (1)$$

and

$$\nabla \times \mathbf{H}_s = (\sigma + i\omega\varepsilon)\mathbf{E}_s + [(\sigma - \sigma_p) + i\omega(\varepsilon - \varepsilon_p)]\mathbf{E}_p. \quad (2)$$

In these equations $\mathbf{E}_s, \mathbf{E}_p$, and \mathbf{E}_t are the scattered, primary and total electric fields, respectively ($\mathbf{E}_t = \mathbf{E}_p + \mathbf{E}_s$), $\mathbf{H}_s, \mathbf{H}_p$, and \mathbf{H}_t are the associated magnetic fields with $\mathbf{H}_t = \mathbf{H}_p + \mathbf{H}_s$, ω is the operating frequency in radians, $i = \sqrt{-1}$, and σ, ε , and μ are the electric conductivity, electric permittivity and magnetic permeability of the medium, respectively, and the subscript 'p' denotes the background or primary value. Note that the terms at the end of each of these equations ($(\mu - \mu_p)\mathbf{H}_p$ and $[(\sigma - \sigma_p) + i\omega(\varepsilon - \varepsilon_p)]\mathbf{E}_p$) are "equivalent source" terms which involve the analytic calculation of the primary electric and magnetic fields that would exist in a whole space of uniform conductivity wherever the properties of the medium are different from that of the background. The boundary conditions employed are Dirichlet conditions, i.e., the tangential component of \mathbf{E}_s is set to zero on the grid boundary. After the scattered fields are determined the total fields are calculated by simply adding the scattered fields to the primary fields.

When both the source and receiver are buried deep within the earth, Newman (1995) has demonstrated that equations (1) and (2) can be solved efficiently for the electric and magnetic fields using iterative Krylov, or more specifically, conjugate gradient methods. However for those models which involve the solution of the fields in the air, it has been our experience that the solution of these first order equations is either slowly or non convergent. This is due to the fact that in the air the conductivity, σ , is practically zero. Thus the first term on the right hand side of equation 2 is very small and the equations numerically decouple. To alleviate this problem we take the curl of equation (1), divide it by μ which allows us to more easily account for variations in the magnetic permeability, and then substitute the resulting equation in (2) to arrive at a vector Helmholtz equation for the electric field;

$$\nabla \times \frac{1}{\mu} \nabla \times \mathbf{E}_s = -i\omega(\sigma + i\omega\varepsilon)\mathbf{E}_s - i\omega[(\sigma - \sigma_p) + i\omega(\varepsilon - \varepsilon_p)]\mathbf{E}_p - i\omega \nabla \times \left[\left(\frac{\mu - \mu_p}{\mu} \right) \mathbf{H}_p \right]. \quad (3)$$

Solution of this equation with Krylov methods is far more efficient than solving equations (1) and (2) simultaneously in the presence of air.

NUMERICAL SOLUTION

The scattered electric and magnetic fields are assigned to each cell using the staggered grid scheme developed by Yee (1966). Following Wang and Hohmann (1993), we have assigned the electric fields to the edges of the cell and the magnetic field to its faces. This yields a finite difference stencil for the solution of the electric field Helmholtz equation as shown in Figure 1.

Thus for node (i,j,k) , the x , y and z components of electric field are sampled at $(i+1/2,j,k)$, $(i,j+1/2,k)$ and $(i,j,k+1/2)$, respectively. Reflections off the boundaries are mitigated by grid stretching, i.e. employing larger cells towards the edges of the mesh.

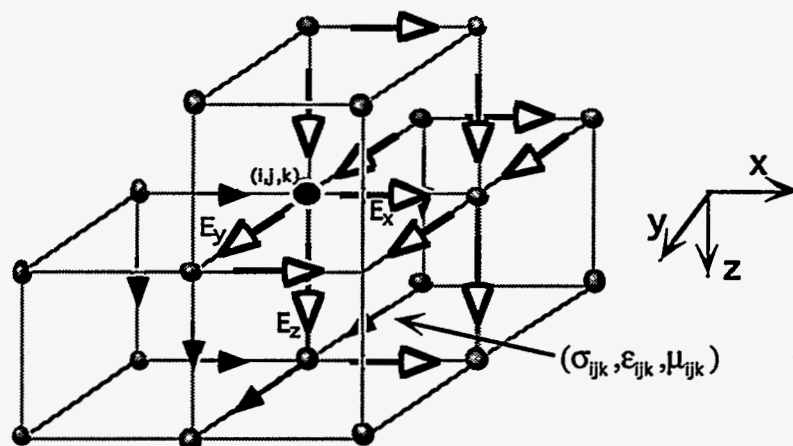


Figure 1 : The staggered grid for the electric field Helmholtz equation. The arrows along the cell edges represent the unknown electric fields needed to form the equations for E_x , E_y and E_z at node (i,j,k) , with the open arrows representing the unknowns needed to form only the equation for E_x . The cell associated with node (i,j,k) contains the corresponding material properties σ, ϵ , and μ .

The above formulation requires that the conductivity, dielectric permittivity and magnetic permeability be computed halfway along a given cell edge in Figure 1. Wang and Hohmann (1993) showed that an average conductivity (and permittivity) can be evaluated by tracing out a line integral of the magnetic field centered on the midpoint of the cell edge. The resulting conductivity is simply a weighted sum of conductivities of the four adjoining cells. Similarly the average magnetic permeability can be derived by enforcing the continuity of tangential \mathbf{B} field across the cell interface. The resulting average is the inverse of the weighted permeability sum for two adjacent cells.

After finite differencing Maxwell's equations for the scattered fields, a linear system is assembled,

$$\mathbf{A}\mathbf{f}=\mathbf{s}, \quad (4)$$

where \mathbf{f} is the unknown vector for the scattered electric field and \mathbf{s} is the equivalent source vector. The matrix \mathbf{A} is sparse with dimension $N \times N$, and it is shown in Smith (1992) how to choose the appropriate scaling factors such that \mathbf{A} becomes complex symmetric.

The solution vector can be obtained using either a bi-conjugate gradient (BICG) or quasi-minimum residual (QMR) (Freund, 1992) technique to iteratively determine the solution within a predetermined error level. These and other Krylov subspace methods effectively find a solution vector which minimizes the difference between the two sides of equation (4) in a least squares sense, i.e., we wish to minimize some form of

$$\mathbf{m} = \|\mathbf{A}\mathbf{f} - \mathbf{s}\|^2. \quad (5).$$

We have chosen to focus on these two Krylov methods as for the type of problem being considered here, they have been determined by Freund to offer the best tradeoff between accuracy and speed. We have extensively tested both routines and determined that although the QMR routine may take slightly longer than the BICG method, it converges in a more stable manner. Thus all results presented here have employed this scheme.

Krylov methods are iterative and for these methods to work effectively, it is often necessary to precondition the system. This process reduces the condition number of the matrix and accelerates convergence (Axelsson and Barker, 1984, pp 28-30). Although we have implemented elaborate preconditioners such as polynomial and incomplete Cholesky decompositions, we have found that simple diagonal or Jacobi scaling (Heroux, Vu and Yang, 1991) provides the quickest solution convergence for our problem even though it may take more iterations. The pre-conditioned system provides for a modified matrix which is still complex symmetric, but with unity on its main diagonal.

Once the scaled version of equation 4 is solved to some desired error, the scaled fields are rescaled back to the true values, after which the fields at the receivers must be calculated. The electric field at the receivers is simply calculated using bi-linear interpolation while the magnetic field is calculated by first taking a numerical approximation of the curl of the electric field on the grid surrounding the receiver and then interpolating the result to the point of interest. (Note: for each frequency both \mathbf{A} and \mathbf{s} must be reformulated, while for different source positions only \mathbf{s} must be recalculated.)

As mentioned in the introduction, the simulation of an airborne survey requires the forward solution for many different source and receiver combinations which can be very time consuming on traditional computers. Therefore the original serial version of the code has been modified to run on massively parallel MIMD (multiple instruction multiple data) machines which can have thousands of processors. These parallel machines are employed by breaking the model up such that each individual processor is in charge of a subset of the model. Because each processor needs only to make the necessary calculations for this subset, and because all of the processors are making their appropriate calculations simultaneously, as the number of processors is increased the solution time is reduced by a factor which is approximately equal to the number employed. To this point the code has been implemented on two different MIMD machines available at Sandia National Laboratories; the 1840 processor Intel Paragon and 1024 processor nCUBE 2. Comparisons against an IBM RS6000 590 workstation has shown a decrease in run times of up to two orders of magnitude. Thus the solution of large, complicated models which were once intractable are now possible.

VERIFICATION OF SOLUTION

To validate the solution, we compare results calculated with it to two other solutions. The first is a semi-analytical half-space solution while the second is a 3-D integral equation solution. In both cases we will employ vertical magnetic dipole sources in the air and measure both the 'x' and 'z' directed magnetic fields.

We begin by considering a 100 Ωm half-space model of variable magnetic permeability. In the first case the permeability is set equal to μ_0 , while in the second case a permeability of $5*\mu_0$ is employed. To achieve the 3-D results, the earth and air are divided into 151,424 cells using a 52 x 52 x 56 grid. This yields a total of approximately $4.5*10^5$ field unknowns to be solved for. To avoid reflections off the mesh boundaries the grid is 580m in length in the x and y directions, and 640m in depth. The source is situated at $x=y=z=290\text{m}$ which is centered in x and y and located 20m in the air above the earth's surface. The frequencies of operation are 0.9, 7.2 and 56 kHz. Eight receivers are in direct line with the transmitter and are positioned at the same height above the earth's surface. The receivers are each separated by 5m with the first receiver situated 5m from the source.

In Figure 2, the 3-D magnetic-field half-space responses arising from the VMD source are plotted against the semi-analytic Hankel transform solution given in Ward and Hohmann (1988, pp. 208-228). Figure 2a shows the results when the magnetic permeability of the half space is set to μ_0 , while in Figure 2b the results for a half space with permeability of $5*\mu_0$ are plotted. For both of the higher frequencies, the comparisons between the 1-D responses and 3-D FD responses are excellent; even those points where the fields change signs achieve similar values. The notable exception is real component of the vertical magnetic field at 900 Hz. We are not able to explain this discrepancy, however it may be due to round-off errors and the small magnitude of this component.

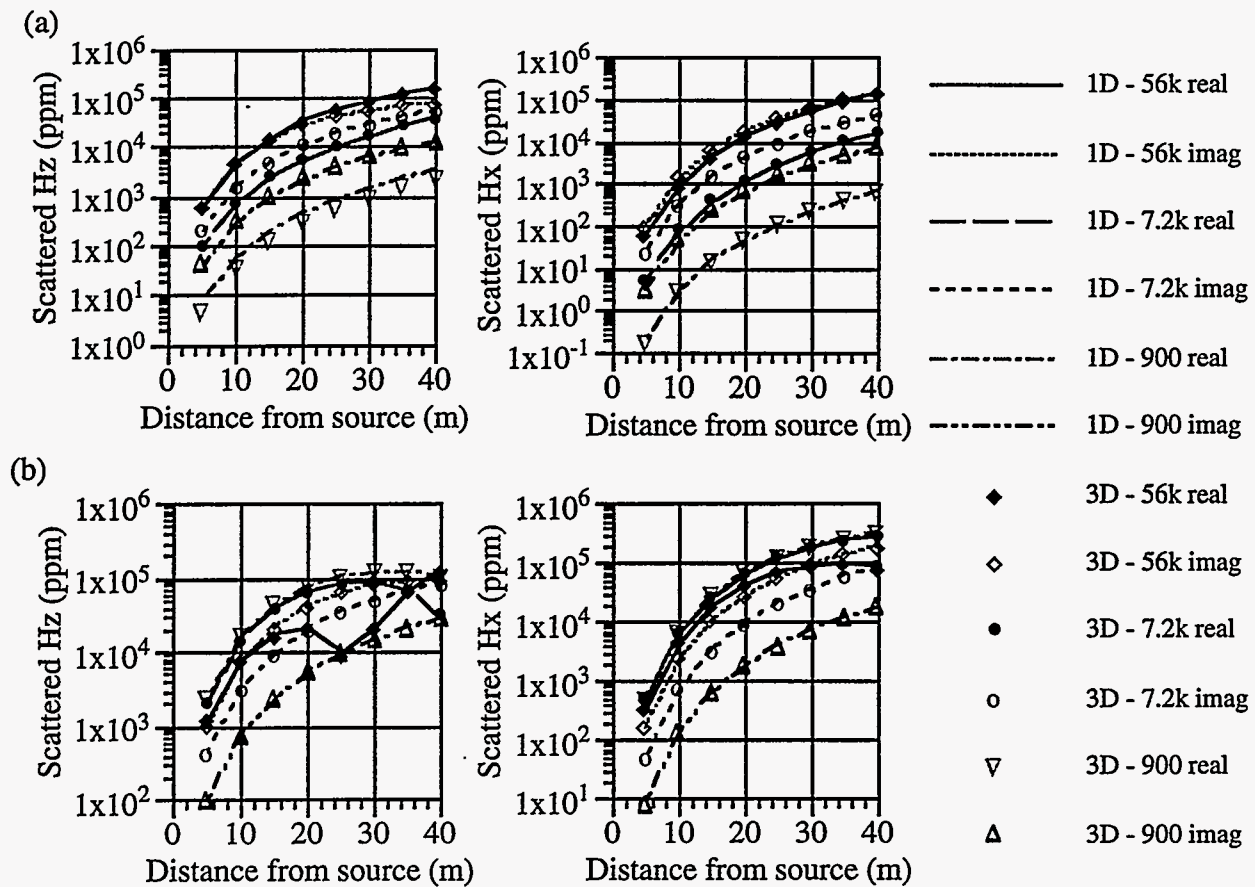


Figure 2 : Comparison of the 3-D results to a 1-D solution. The scattered fields are plotted in parts-per-million of the free space field. a) Comparison for $\mu=\mu_0$. b) Comparison for $\mu=5*\mu_0$.

In this case as well as all following examples we arbitrarily chose a residual error (equation 4 normalized by $\|s\|^2$) of 10^{-8} to designate the point at which the solution had converged to an acceptable accuracy. Table 1 shows the number of iterations, and the cpu time required to reduce the squared error to this level for two different machines: 1) an IBM RS-6000 590 which is a high end workstation, and 2) the 1840 processor Intel Paragon. Due to the relatively small size of the problem, only 125 processors were employed on the Paragon. However, even though a limited number of processors are employed, the Paragon is still 10 times faster the IBM. Thus the necessity of using this type of machine to model airborne surveys where thousands of source positions may be employed is evident. The second thing to notice is that as the frequency is increased, the solution converges faster. We have found this to be true until the MHz range is reached at which point the dielectric properties become a factor.

In our next check, we simulate the HEM response of a 3-D body using the 3-D FD code and compare the results to those of an IE solution (Newman et al., 1986). Consider the 3-D model shown in Figure 3 which is designed to crudely simulate a buried pit which has been filled with a conductive material such as brine. The body has a resistivity of $1 \Omega\text{m}$ and is embedded in a $100 \Omega\text{m}$ half-space. Its dimensions are 4m in depth extent, 10m wide with a strike length of 20 m, and it is buried at 2 m depth. Again the flight line is 20 m above the earth surface, and a VMD source is used to excite the body at 7.2 and 56 kHz. The transmitter and receiver are separated by a fixed distance of 8 m, with the receiver leading the transmitter to the right. Results have been plotted

halfway between the transmitter and the receiver along the flight line where this line bisects the body.

Frequency (kHz)	Half Space $\mu=\mu_0$				Half Space $\mu=5*\mu_0$			
	IBM RS600 590		Intel Paragon		IBM RS600 590		Intel Paragon	
	Iteration	Time (s)	Iteration	Time (s)	Iteration	Time (s)	Iteration	Time (s)
0.9	1009	1282	1039	129	1150	1465	1167	42
7.2	605	770	605	75	651	828	660	82
56	586	745	587	73	346	441	342	145

Table 1 - Comparison of solution times for the half-space model on the IBM RS600 590 and the Intel Paragon.

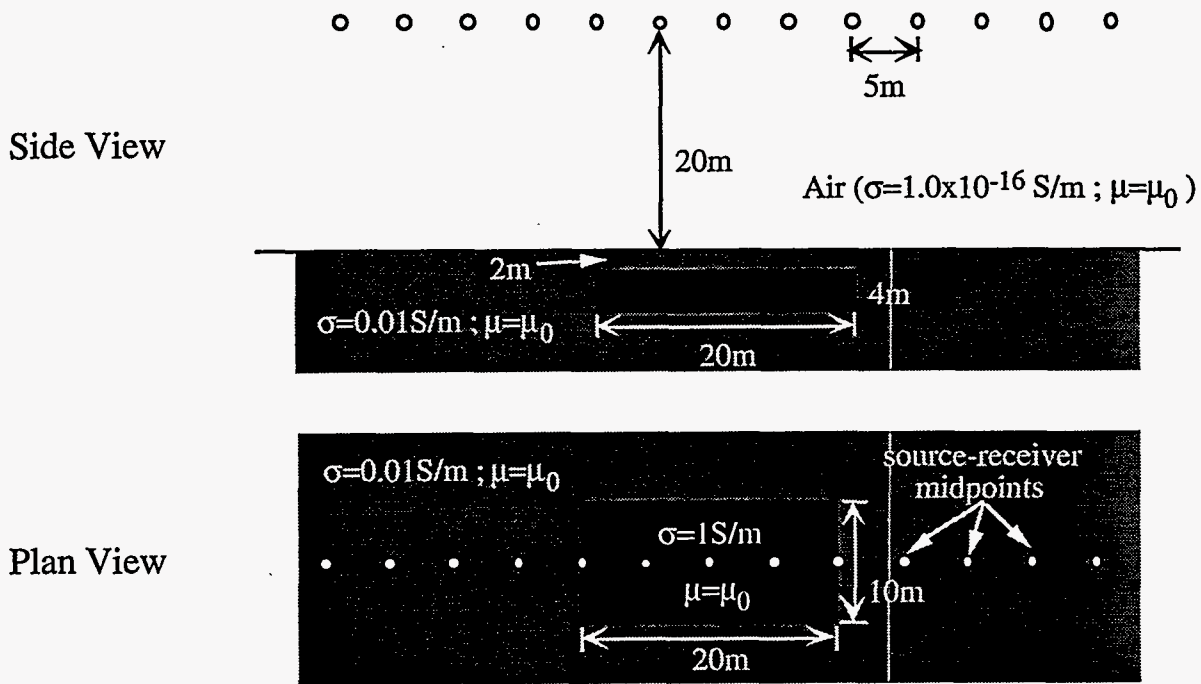


Figure 3 : The 3-D model employed to compare the finite difference and integral equation solutions.

Comparisons between the vertical and horizontal magnetic fields for the 3-D model shown in Figure 3 (the body is centered at 0 m along the profile) are shown in Figure 4. Here as in Figure 2 the free space response of the transmitter has been removed and the remaining components plotted in parts per million of this primary field (PPM). Overall the comparisons of the fields are very good, especially in the vertical components where the error between the two solutions is approximately 1.3% in amplitude for the 56kHz simulation, and 2.4% for the 7.2 kHz results. The results do not compare quite as well for the horizontal components with a maximum error of 7.3% for the 56kHz simulation and 9.3% at 7.2kHz. However, due to the order of magnitude better comparisons that were achieved for the half-space model in Figure 2, and the excellent comparison for the vertical fields, we feel that the finite difference code is well within the accuracy limits needed for modeling the airborne response of environmental targets.

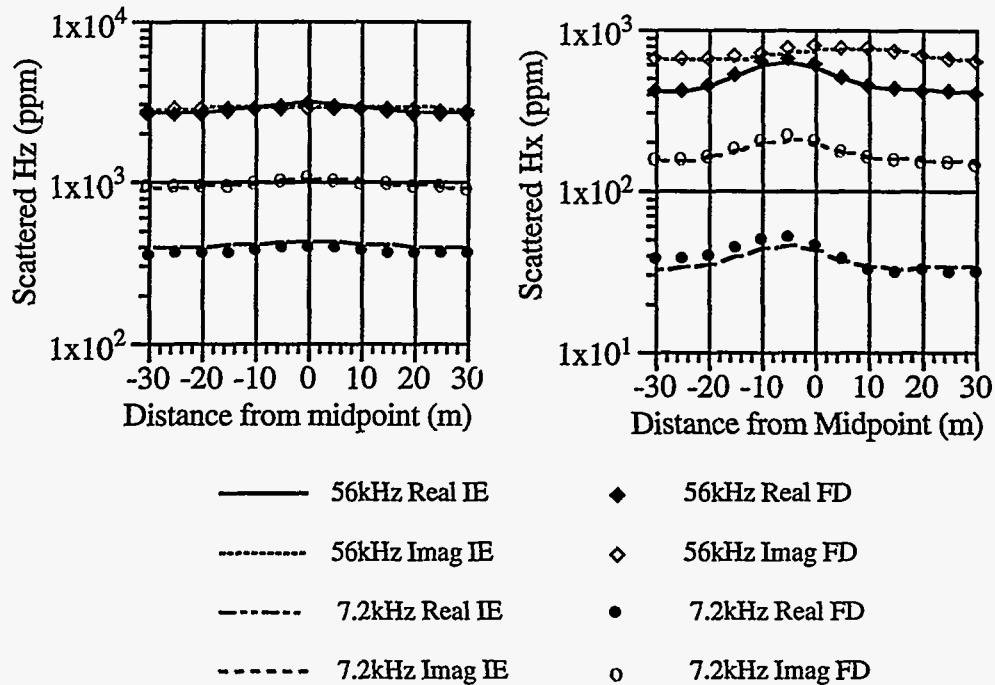


Figure 4 : Comparison of the 3-D integral equation (IE) and finite difference (FD) solutions.

SIMULATION OF THE FLORIDA EVERGLADES SURVEY

In order to determine how far inland sea water has intruded into the Florida Everglades, the United States Geological Survey and DIGHEM flew a HEM survey over the region in the summer of 1994 as part of the Department of Interior's "South Florida Ecosystem Initiative". Figure 5 shows the 7.2 kHz and 0.9 kHz coplanar data in terms of apparent resistivity that were collected across the fresh water-salt water contact. In this area the flight line was essentially perpendicular to this contact. Notice that the 7.2 kHz data produce higher apparent resistivities compared to the 0.9 kHz data indicating the subsurface becomes more conductive with depth. Although 1-D inversions along the line would be able to give a good estimate of the surface and deeper conductivities, it would not accurately estimate the 3-D nature of the interface and thus, the 3-D finite difference code was employed.

Figure 7 shows a x-z crosssection through the model at the central position in y. This 1.6 km section corresponds to the same section for which the data have been plotted. The model was divided into 208 x 36 x 66 cells which yields a total of 1.48×10^6 unknowns to solve for. Notice that this is much too large of a model to solve for on our IBM machine; it can handle a maximum of approximately 6×10^5 unknowns. A total of 27 source-receiver positions were employed at 60m intervals and a fine discretization has been employed at these locations to accurately calculate the scattered fields. In between these positions a coarser discretization has been employed to reduce the size of the model. The resistivities in the subsurface range from $140 \Omega\text{m}$ on the left hand side of the model to $10 \Omega\text{m}$ at depth. It must be pointed out that because of the limited amount of data employed in this simulation, this model is non-unique. Thus we are not trying to fit the data exactly, but rather design a simple model which reproduces the general features observed in the data.

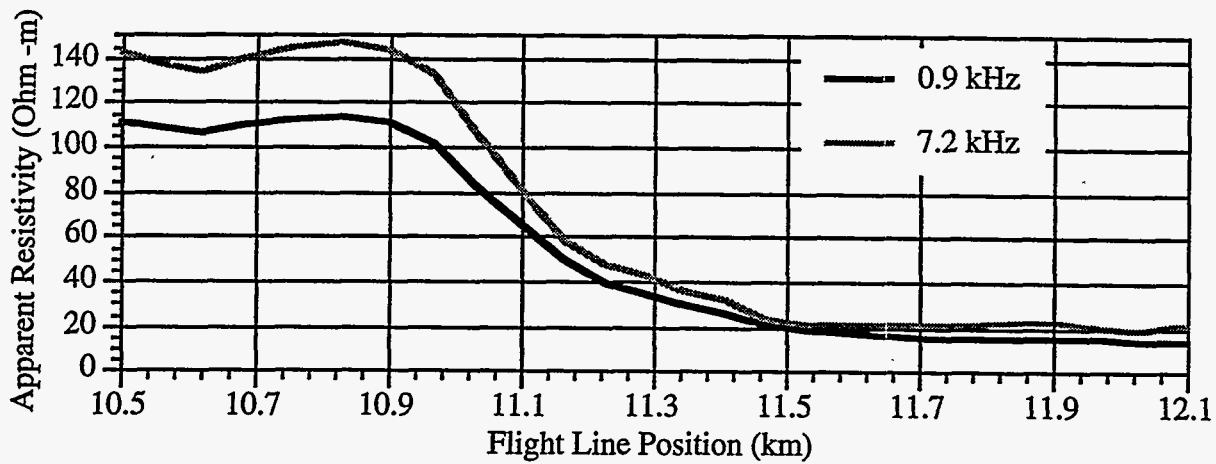


Figure 5 : A portion of the data collected on flight line 10070 of the Florida Everglades HEM survey.

Figure 6 shows the results from the simulation, which took approximately 3 hours to run on the Paragon with 384 processors. Notice that the 0.9 kHz results fit the data in Figure 5 very well. The 7.2 kHz data however, seems to produce apparent resistivities that are a little high from 600 m to 1200 m. This seems to indicate that in this region, the near surface of the model may be too resistive. However, we found the shapes of these curves to be very sensitive to the dip of the interface as well as the thickness of the surficial layers. Thus we feel that this model gives a good general representation of the geometry that is producing the results measured at this location.

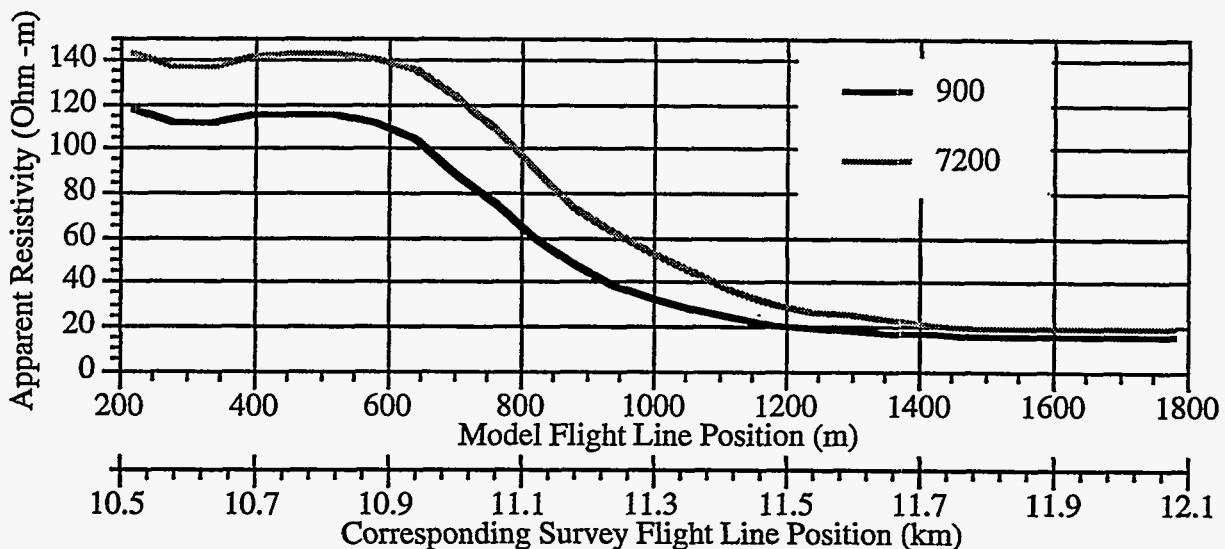


Figure 6 : Results from the Everglades simulation shown in Figure 7.

CONCLUDING REMARKS

A 3-D frequency domain EM modeling code has been implemented for HEM simulations. The Helmholtz equation for the electric fields is approximated using finite differences on a staggered grid and to avoid numerical instabilities, the problem is formulated in terms of the scattered rather than total electric fields. This definition allows us to replaced the impressed source with an equivalent source which possesses a much smoother spatial dependence. After finite differencing, a complex-symmetric matrix system of equations is assembled and scaled before it is

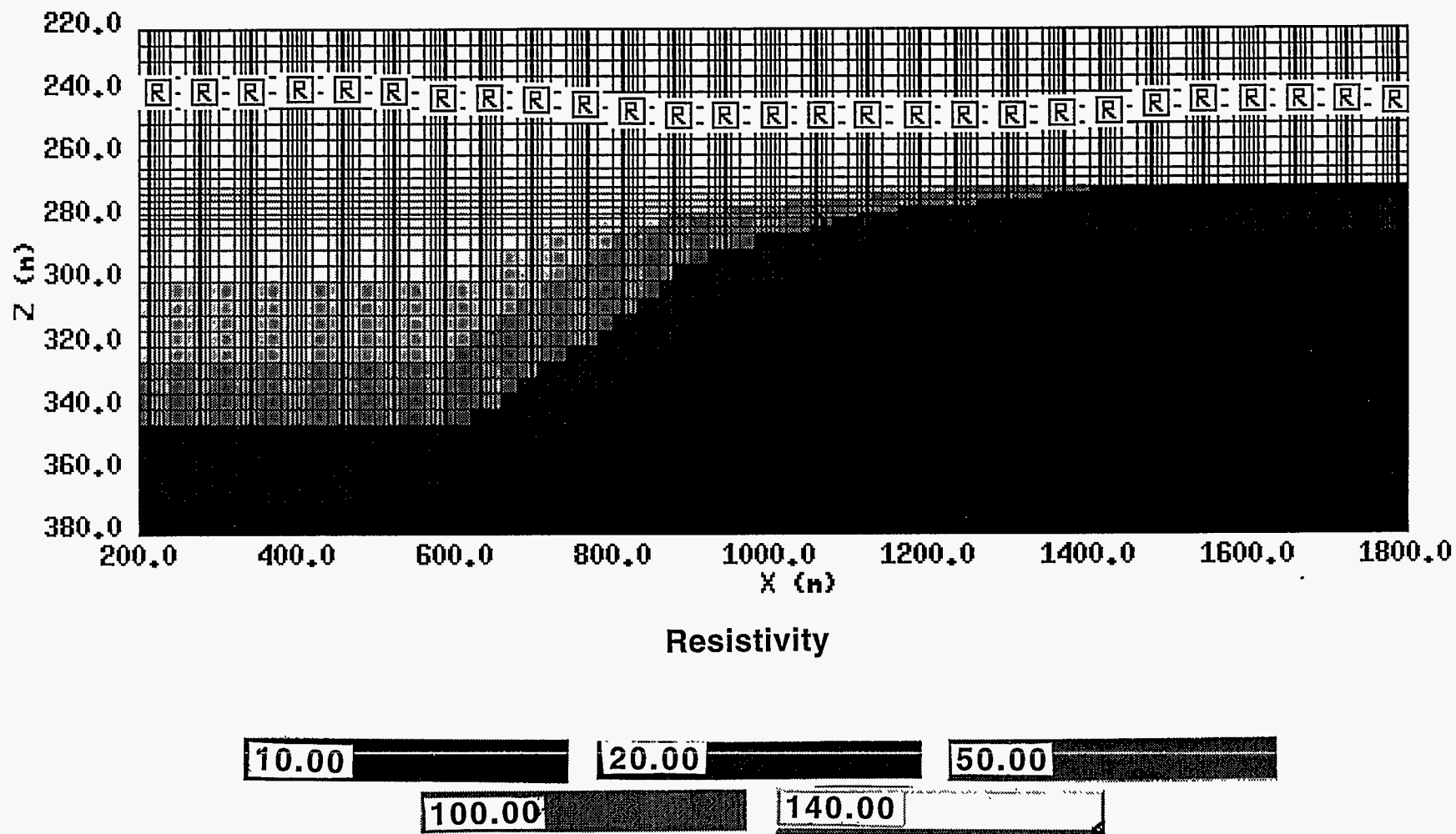


Figure 7 : Central portion of the model employed to simulate flight line 10070 of the Florida Everglades survey. The model stretches from 0 to 2000 m in the x direction, 0 to 440 m in the y direction and 0 to 630 m in the z direction. The flight line is located at $y=220\text{m}$, and the air-earth interface is at $z=270\text{m}$. The vertical exaggeration is 4 times the horizontal. The R's designate the receiver position with the sources located 8m to the left.

solved using the QMR method. We have employed the QMR method since it was judged to be one of the best available Krylov subspace method for solving matrix systems that are complex symmetric. The modeling code has been compared against a variety of 1-D and 3-D numerical models and was found to produce results in that are in good agreement. Implementation on a massively parallel computer architecture allows us to simulate HEM responses that are computationally intractable on normal serial computers. This added versatility has been demonstrated with a simulation of a survey conducted in the Florida everglades.

In the near future we will be applying the code to more complicated surveys, such as the one conducted at Oak Ridge National Laboratory in Tennessee. In these cases structures such as dipping layers and the effects of topography will be simulated in order to help in the interpretation. In the long range we plan to employ this code as the forward solver within a 3-D inversion routine. This further modification will help in the interpretation of airborne data in that it will remove some of the problems associated with simpler inversion schemes such as 1-D inversions.

ACKNOWLEDGMENTS

We express our thanks to Ki Ha Lee of Lawrence Berkeley Laboratory for the 1-D layered-earth code used in our comparisons. Also we would like to thank the geophysics branch of the USGS for providing the Florida Everglades data. This work was performed at Sandia National Laboratories, which is operated for the U.S. Department of Energy (DOE). Funding for this work was provided by DOE's office of Basic Energy Sciences, Division of Engineering and Geoscience under contract DE-AC04-94AL85000.

REFERENCES

- Alumbaugh, D. L., and Newman, G. A., 1994, Fast frequency domain electromagnetic modeling using finite differences: 64th Ann. Internat. Mtg., Soc. Explor. Geophys., Expanded Abstracts, 369-373.
- Ashby, S.F., Manteuffel, T.A. and Saylor, P.E., 1990, A taxonomy for conjugate gradient methods: *SIAM J. Numer. Anal.*, **27**, 1542-1568.
- Axelsson, O., and Barker, V.A., 1984, Finite element solution of boundary value problems: Theory and Computation, Academic Press Inc.
- Freund, R., 1992, Conjugate gradient type methods for linear systems with complex symmetric coefficient matrices: *SIAM J. Sci. Statist. Comput.*, **13**, 425-448.
- Heroux, M. A., Vu, P. and Yang C., 1991, A parallel preconditioned conjugate gradient package for solving sparse linear systems on a Cray Y-MP: *Applied Numerical Mathematics*, **8**, 93-115.
- Newman, G. A., Hohmann, G. W. and Anderson, W. L., 1986, Transient electromagnetic response of a three-dimensional body in a layered earth: *Geophysics*, **51**, 1608-1627.
- Newman, G. A., 1995, Cross well electromagnetic inversion using integral and differential equations: *Geophysics*, May-June issue (in press).
- Palacky, G. J. and West, G. F., 1991, Airborne electromagnetic methods: in *Electromagnetic Methods in Applied Geophysics V2.*, part b Application:, Nabighian, M. N., Ed., 811-879
- Smith, T. J., 1992, Conservative modeling of 3-D electromagnetic fields: International Association of Geomagnetism and Aeronomy, 11th Workshop on Electromagnetic Induction in the Earth, Wellington, New Zealand, Meeting Abstracts.
- Tripp, A.C., and Hohmann, G. W., 1984, Block diagonalization of the electromagnetic impedance matrix of a symmetric buried body using group theory: *Inst. of Electr. and Electron. Eng., Trans. Geoscience and Remote Sensing*, **GE-22**, 62-69.
- Wang T. and Hohmann, G. W., 1993, A finite difference time-domain solution for three-dimensional electromagnetic modeling: *Geophysics*, **58**, 797-809.
- Ward, S.H., and Hohmann, G.W., *Electromagnetic theory for geophysical applications: in Electromagnetic Methods in Applied Geophysics: V1.*, Theory, Nabighian, M. N., Ed., 130-311.
- Xiong, Z., 1992, Electromagnetic modeling of 3-D structures by the method of system iteration using integral equations: *Geophysics*, **57**, 1556-1561.
- Yee, K. S., 1966, Numerical solution of initial boundary problems involving Maxwell's equations in isotropic media: *IEEE Trans. Ant. Prop.*, **AP-14**, 302-309.

DISCLAIMER

This report was prepared as an account of work sponsored by an agency of the United States Government. Neither the United States Government nor any agency thereof, nor any of their employees, makes any warranty, express or implied, or assumes any legal liability or responsibility for the accuracy, completeness, or usefulness of any information, apparatus, product, or process disclosed, or represents that its use would not infringe privately owned rights. Reference herein to any specific commercial product, process, or service by trade name, trademark, manufacturer, or otherwise does not necessarily constitute or imply its endorsement, recommendation, or favoring by the United States Government or any agency thereof. The views and opinions of authors expressed herein do not necessarily state or reflect those of the United States Government or any agency thereof.